

Investigation of carbonaceous compounds deposited on NiMo catalyst used for ultra-deep hydrodesulfurization of gas oil by means of temperature-programmed oxidation and Raman spectroscopy

Naoto Koizumi^a, Yoshihisa Urabe^a, Kazuhiro Inamura^b,
Takashi Itoh^c, Muneyoshi Yamada^{a,*}

^a Department of Applied Chemistry, Graduate School of Engineering, Tohoku University, 6-6-07, Aramaki, Aoba-ku, Sendai 980-8579, Japan

^b Central Research Laboratories, Idemitsu Kosan Co., Ltd., 1280 Kami-izumi, Sodegaura, Chiba 299-0293, Japan

^c Center for Interdisciplinary Research, Tohoku University, 6-3 Aramaki, Aoba-ku, Sendai 980-8578, Japan

Abstract

NiMo/Al₂O₃ catalyst used for ultra-deep HDS of several gas oils at various conditions was characterized by both temperature-programmed oxidation combined with mass spectroscopy (TPO–MS) and/or gas chromatography (TPO–GC), and Raman spectroscopy to make clear how the catalyst was deactivated. TPO–MS showed the presence of carbonaceous compounds containing H and N atoms on the used catalysts. TPO–GC showed that the combustive property of the carbonaceous compounds sensitively changes depending on the HDS reaction conditions and the position of the catalyst charged in the HDS reactor. A curve fitting analysis of TPO–GC profiles indicated that the carbonaceous compounds combusted below 680 K during TPO were observed on all the spent catalysts examined here whereas more refractory carbonaceous compound (combusted at around 690 K during TPO) was observed on the catalyst that had experienced severe HDS reaction conditions. More refractory carbonaceous compound was preferentially observed on the catalyst charged near the outlet of the HDS reactor. Raman spectra of the carbonaceous compounds indicated that the carbonaceous compounds combusted below 680 K during TPO has an amorphous-like structure whereas the refractory carbonaceous compound has a graphite-like one. Raman spectra also indicated that the graphite-like carbonaceous compound possesses a greater lateral size than the amorphous-like one, implying that the refractory carbonaceous compound can cover the catalyst surface more effectively. The carbonaceous compound having a graphite-like structure is one of main reasons for the catalyst deactivation. It is suggested that the precursor for this type of carbonaceous compound is not formed directly from the feed, but indirectly formed during the HDS of gas oil, because of its preferential deposition on the catalyst charged near the outlet of the HDS reactor.

© 2005 Elsevier B.V. All rights reserved.

Keywords: Catalyst deactivation; Ultra-deep HDS; Carbonaceous compound; TPO; Raman spectroscopy

1. Introduction

Because of severe regulations for the emission from diesel vehicles, ultra-deep hydrodesulfurization (HDS) of gas oil currently becomes an important issue. For example, the sulfur content of gas oil in Japan is regulated below 50 mass ppm-S at present and is decided to be below 10 mass ppm-S in a new regulation that will be brought into

operation from 2007. Therefore, great effort has been made to develop the catalyst effective for ultra-deep HDS of gas oil. It has been in consequence found that NiMo-based catalysts show higher activities for the HDS of refractory sulfur compounds such as 4,6-dimethyldibenzothiophene [1]. However, it has been also found that this type of catalyst is seriously deactivated during ultra-deep HDS of gas oil, especially at the beginning of on-stream [2]. Therefore, it is an important research theme in this field to suppress the deactivation of NiMo catalyst. Nevertheless, little has been known about the deactivation mechanism of NiMo catalyst

* Corresponding author. Tel.: +81 22 795 7214; fax: +81 22 795 7293.

E-mail address: yamada@erec.che.tohoku.ac.jp (M. Yamada).

under the reaction conditions typically employed for ultra-deep HDS of gas oil.

In the heavy oil processing, carbonaceous compounds deposited during the reaction are thought to be one of important causes for the catalyst deactivation [3,4]. Therefore, various kinds of characterization techniques have been utilized to make clear the structure and chemical nature of the carbonaceous compounds deposited on the spent catalyst. Among these techniques, temperature-programmed oxidation combined with MS spectroscopy and/or gas chromatography (TPO–MS and/or TPO–GC) can determine the amount of the carbonaceous compounds precisely and discriminate minute variations in combustive property of the carbonaceous compounds, which may be related with the reactivity of the carbonaceous compounds under the HDS reaction conditions. Thus, this technique has a potential for providing quantitative insight into the impact of the carbonaceous compounds upon the catalyst deactivation. So far, several authors have reported TPO–MS profiles of the carbonaceous compounds deposited on NiMo catalysts used for the HDS of straight run gas oil (SRGO) [5], vacuum gas oil (VGO) [6,7,8] and heavy petroleum fraction [9]. However, the carbonaceous compounds on the NiMo catalyst used for the ultra-deep HDS of gas oil have never been investigated by TPO techniques yet.

Recently, the authors [10] investigated the nature and the amount of carbonaceous compounds deposited on NiMo catalyst used for ultra-deep HDS of gas oil in a bench-scale plant by TPO–MS and TPO–GC. TPO–GC combined with a curve fitting analysis sensitively probed the combustive property of carbonaceous deposits and showed that at least two or three types of carbonaceous compounds having different combustive properties are deposited on the spent catalysts depending on the reaction conditions employed for ultra-deep HDS of gas oil. Furthermore, it was found that the residual HDS activity of the spent catalyst decreases with increasing the amount of a refractory carbonaceous compound. Based on these results, we suggested that the deposition of the refractory carbonaceous compound is one of main reasons for the catalyst deactivation. However, TPO technique does not always provide information about the carbonaceous compounds as they are because the structure of the deposited carbonaceous compound may be changed during TPO measurement. Furthermore, it is difficult to connect the combustive property of carbonaceous compounds with their structure because TPO may involve complex surface reactions as is pointed out in the previous studies [11,12]. Therefore, it is indispensable to investigate the carbonaceous compounds by a non-destructive technique as well as TPO technique.

Raman spectroscopy has been extensively utilized as a characterization technique for carbon materials because it can probe the graphitization degree and the morphology of the carbon materials sensitively. Besides, Raman spectrum can be obtained at ambient conditions. Therefore, it is expected that the combination of TPO technique and Raman

spectroscopy becomes a powerful tool for the characterization of the carbonaceous compounds deposited on the spent catalyst. It is worthy to note here that Raman spectrum of the carbonaceous compound deposited on the catalyst used for ultra-deep HDS of gas oil is never found in the previous studies. Therefore, the present study has characterized the carbonaceous compound deposited on NiMo catalysts that had been used for ultra-deep HDS of several gas oils at various conditions by TPO–GC (MS) and Raman spectroscopy. Based on obtained results, we will discuss the structure of the carbonaceous compound in relation to the catalyst deactivation and its formation mechanism.

2. Experimental section

2.1. Spent catalysts

Four types of fresh NiMo/Al₂O₃ catalysts (denoted as NiMo-A, NiMo-B, NiMo-C and NiMo-D catalysts for the clarification) were prepared by Idemitsu Kosan Co. Ltd. These catalysts include 6 mass% NiO and 30 mass% MoO₃ in the fresh state. P₂O₅ (3 mass%) is also included in the fresh catalyst as an additive.

These catalysts were subjected to the ultra-deep HDS of several gas oils in a bench-scale fixed bed reactor at various reaction conditions. Reaction conditions including the maximum reaction temperature, H₂ partial pressure and days on-stream are summarized in Table 1 as well as the operation mode employed for the HDS reaction. After the HDS reaction, the spent catalyst was drawn out of the reactor and then stored in a bottle filled with gas oil. In the case of NiMo-B, NiMo-C and NiMo-D catalysts, the spent catalysts were separated from near the inlet and outlet of the HDS reactor whereas the spent NiMo-A catalysts were a mixture of them. According to the reaction conditions and the position of the catalyst charged in the HDS reactor, total nine types of the spent catalyst were examined by TPO and Raman spectroscopy. Before TPO and Raman measurements, residual gas oil was removed from the spent catalyst by Soxhlet extraction followed by drying in air at 393 K for 12 h.

Table 1
Operation mode and reaction conditions employed for the ultra-deep HDS of gas oils with NiMo catalysts

Spent catalyst	Operation mode (ppm-S)	<i>T</i> _{max} (K) ^a	H ₂ p.p. (MPa) ^b	Days on stream
NiMo-A				
(i)	50	583	5.0	2
(ii)	50	633	5.0	15
(iii)	50	618	5.0	170
NiMo-B	10	618	5.0	170
NiMo-C	10	645	5.0	110
NiMo-D	10	632	5.0	200

^a Maximum reaction temperature.

^b H₂ partial pressure.

2.2. TPO measurements

TPO of the spent catalyst was performed with a conventional fixed bed reactor connected with online GC (Shimadzu Co., GC2010) and GC/MS (Shimadzu Co., QP5000). 0.05 g of the dried and sieved spent catalyst with a particle size from 150 to 250 μm was charged in a quartz reactor (i.d.: 4 mm, length: 250 mm) and then heated in a stream of 10% O_2/He (purity > 99.99995%) from 303 to 1023 K at the heating rate of 5 K min^{-1} . Products formed during TPO were detected with the online GC and/or GC/MS. The online GC is equipped with three sensitive and selective detectors, i.e. flame ionization detector (FID), flame photometric detector (FPD) and flame thermionic detector (FTD). The effluent gas from the reactor is divided into three parts and each part is connected with one of these detectors. On the way to FID, a methanizer was set in order to convert the formed CO_x into CH_4 with a reduced Ni catalyst.

2.3. Raman measurements

Raman spectrum of the carbonaceous compounds deposited on the spent catalysts was measured with a homemade spectrometer equipped with p-polarized Ar^+ laser (514.5 nm, 40 mW) as an excited source. The dried spent catalyst was ground into fine powder with a mortar and pestle and subjected to Raman measurement at an ambient temperature. The obtained spectrum was deconvoluted with Lorentz-type peaks to determine accurate band positions, band intensities and full widths at half maximum (FWHM).

3. Results and discussion

3.1. TPO profiles of spent NiMo-A catalyst

In the present paper, we will mention at first the combustive property and the amount of carbonaceous compounds deposited on the spent NiMo-A catalysts investigated by TPO. Although TPO results of the spent NiMo-A catalysts are already reported in our previous paper [10], it is important to present them here again for understanding the meaning of findings in the present study more clearly.

During TPO of the spent NiMo-A catalysts, H_2O , CO_x , SO_2 and small amount of CH_3CN [10] were detected during TPO–MS. NO_x was not detected at all although several authors reported that NO_x is detected during TPO of the catalysts that had been used for the heavy oil processing [5,8,12]. Fig. 1 shows typical CO_x , CH_3CN and SO_2 formation profiles during TPO–GC of the spent NiMo-A (i) catalyst. These products are detected with FID combined with the methanizer, FTD and FPD, respectively. Broad peaks are clearly observed in both CO_x and CH_3CN profiles. These peaks are asymmetric and seem to be superimposed

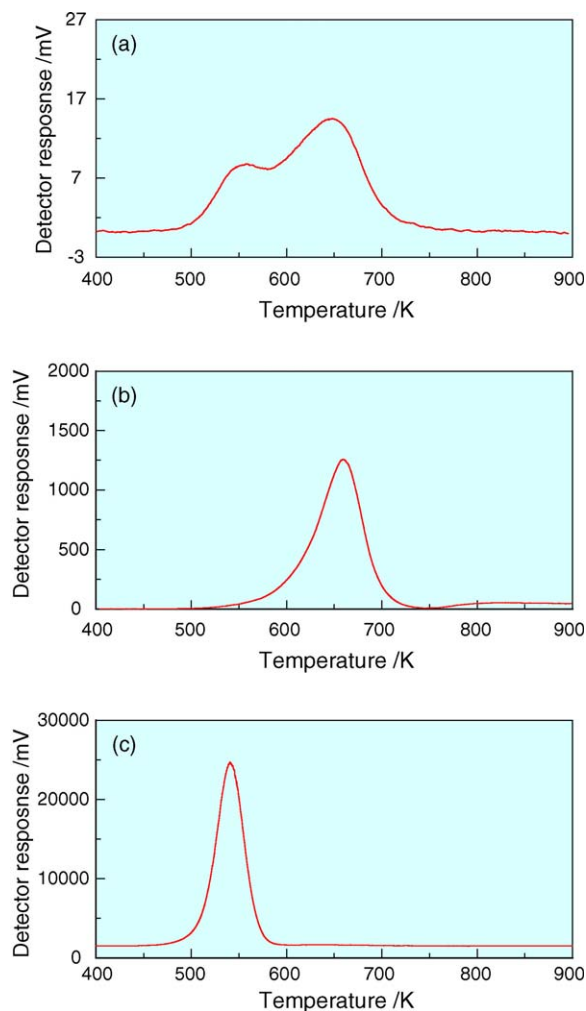


Fig. 1. CO_x (a), CH_3CN (b) and SO_2 (c) formation profiles during TPO of the spent NiMo-A (i) catalyst used for ultra-deep HDS of gas oil.

upon several symmetric peaks. From these profiles, it can be said that the carbonaceous compounds deposited on this catalyst contain N atoms as well because CH_3CN peak overlaps CO_x peak in a wide range. On the other hand, a relatively sharp and symmetric peak appears at lower temperature (around 550 K) in SO_2 formation profile. Because a similar SO_2 peak was observed during TPO of the fresh catalyst sulfided in a stream of 5% $\text{H}_2\text{S}/\text{H}_2$ at 673 K, this peak is assigned to the oxidation of the Ni and Mo sulfides.

Fig. 2 compares CO_x formation profiles during TPO–GC of spent NiMo-A (i) and NiMo-A (iii) catalysts that had been used for ultra-deep HDS of gas oils at different reaction conditions. The spent NiMo-A (iii) catalyst had been experienced a higher reaction temperature and longer days on-stream, and thus deactivated more severely. The total amount of carbonaceous compound deposited on these spent catalysts was calculated from the total area of CO_x formation profiles and are summarized in Table 2. From this table, we can see that the total amount of carbon on these spent catalysts is almost the same. However, CO_x formation profile

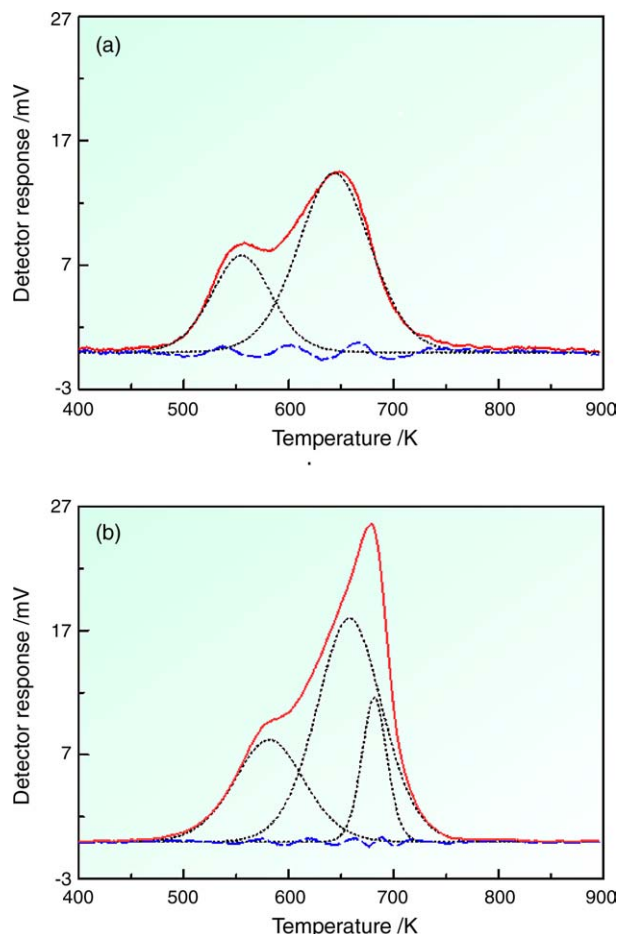


Fig. 2. CO_x formation profiles during TPO of the spent NiMo-A (i) (a) and NiMo-A (iii) (b) catalysts used for ultra-deep HDS of gas oil at different reaction conditions. Curve-fitting results for each profile are also shown in the same figure ((—) observed, (---) fitted and (---) difference).

Table 2
Amount of carbonaceous compounds deposited on the spent NiMo catalysts

Spent catalyst	Total ^a	Curve fitting results ^{a,b}		
		I ^c	II ^c	III ^c
NiMo-A				
(i)	8.2	2.6	5.6	0
(ii)	10.7	3.2	6.3	1.1
(iii)	10.8	3.0	6.2	1.5
NiMo-B				
Inlet	6.2	2.4	3.8	0
Outlet	7.0	2.6	2.6	1.7
NiMo-C				
Inlet	6.8	2.3	4.0	0.5
Outlet	9.7	2.4	6.3	1.0
NiMo-D				
Inlet	5.0	2.1	1.9	1.1
Outlet	7.5	2.1	3.8	1.6

^a The amount of carbonaceous compounds is shown here as C-mmol g cat^{-1} .

^b Curve fitting results show the amount of carbonaceous compounds having different combustive properties.

^c The Roman numerals represent the deconvolved peaks. They are denoted as I, II and III from low temperature to high temperature.

of these two catalysts is obviously different from each other. Curve-fitting analyses of CO_x formation profiles show that these profiles can be fitted with two or three Gauss–Lorentz type peaks (see Fig. 2). In the profile for the spent NiMo-A (iii) catalyst, the third peak appears at around 690 K that is never observed in the profile for the spent NiMo-A (i) catalyst. From the analyses of CO_x formation profiles of other spent NiMo-A catalysts, it was found that two peaks always appeared below 680 K whereas another peak was observed in the range from 680 to 690 K if ultra-deep HDS of gas oil was performed above 600 K. Therefore, at least two types of carbonaceous compounds having different combustive properties are observed on all the spent NiMo-A catalyst whereas more refractory carbonaceous compound is also observed depending on the reaction conditions. The amount of the refractory carbonaceous compound is about 10% of the total amount of the carbonaceous compounds on C-mol basis in the case of the spent NiMo-A (iii) catalyst as shown in Table 2. The amount of the refractory carbonaceous compound increased with increasing both 90% distillation temperature of the feed gas oil and the maximum reaction temperature whereas no clear relationship was observed between the amount of the refractory carbonaceous compound and the days on-stream (from 2 to 170 days) [10].

3.2. TPO profiles of spent NiMo catalyst charged near the inlet and outlet of the HDS reactor

In the fixed bed reactor, the reaction atmosphere changes during ultra-deep HDS of gas oil depending on the position of the catalyst charged in the reactor because several reactions proceed along with the axis of the reactor. This may cause some differences in the properties of carbonaceous compounds on the spent catalysts. In order to make clear this point, we then investigated and compared combustive properties of carbonaceous compounds on the spent catalyst charged near inlet and outlet of the HDS reactor by TPO–GC.

Figs. 3 and 4 show CO_x formation profiles during TPO–GC of spent NiMo-B and NiMo-C catalysts. These catalysts have a similar composition as catalytic materials. The spent NiMo-C catalyst suffered from more severe deactivation because this catalyst had been used for ultra-deep HDS of heavier gas oil. Total amount of carbonaceous compounds on these spent catalysts is also summarized in Table 2. In the case of the spent NiMo-B catalyst, the total amount of carbonaceous compounds remains constant irrespective of the position of the catalyst in the HDS reactor. However, CO_x formation profile greatly differs. The curve fitting analyses reveal that CO_x formation profile for the catalyst charged near the inlet of the reactor shows two broad peaks below 680 K whereas a relatively sharp peak also appears at around 690 K in the profile for the catalyst charged near the outlet of the reactor. It is worthy to note that the peak at around 690 K is similar to that observed in the profile for spent NiMo-A (iii) catalyst. On the other hand, CO_x

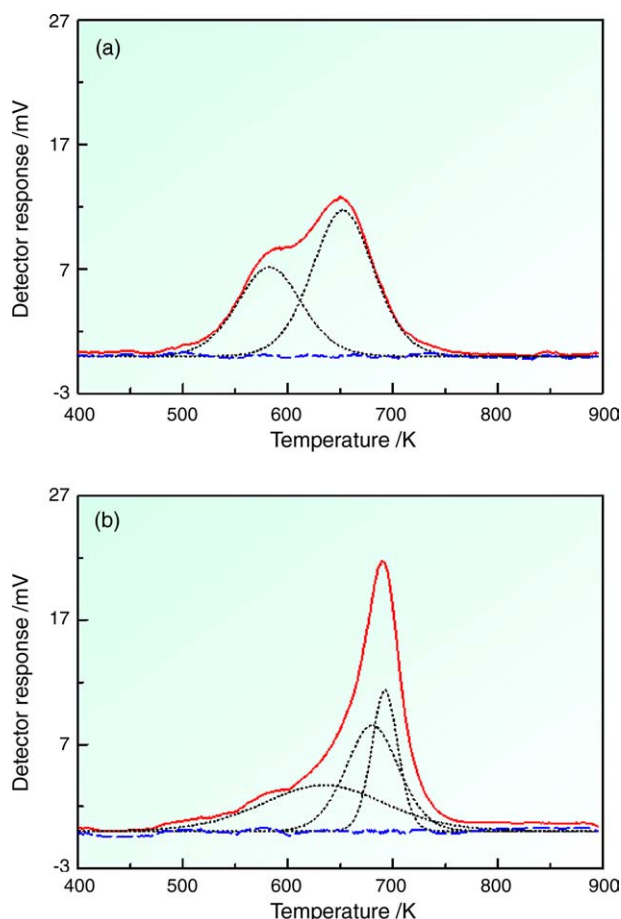


Fig. 3. CO_x formation profiles during TPO of the spent NiMo-B catalyst charged near the inlet (a) and the outlet (b) of the HDS reactor. Curve-fitting results for each profile are also shown in the same figure ((—) observed, (---) fitted and (---) difference).

formation profiles for the spent NiMo-C catalysts charged near both the inlet and outlet of the HDS reactor are fitted three Gauss–Lorentz type peaks and the third peak appears at 680–690 K in both profiles. Therefore, the refractory carbonaceous compound is deposited on the spent NiMo-C catalyst irrespective of its bed position in the HDS reactor although the amount of the refractory carbonaceous compound is greater if the catalyst was charged near the outlet of the HDS reactor (see Table 2). CO_x formation profile for the spent NiMo-D catalyst was similar to that for the spent NiMo-C catalyst. These results clearly show that the deposition of the refractory carbonaceous compound strongly depend on the catalyst bed position in the HDS reactor. This carbonaceous compound is preferentially observed on the catalyst charged near the outlet of the HDS reactor.

3.3. Raman spectra of carbonaceous compounds deposited on spent NiMo catalyst

To get structural information about the carbonaceous compounds deposited on the spent NiMo catalyst, the

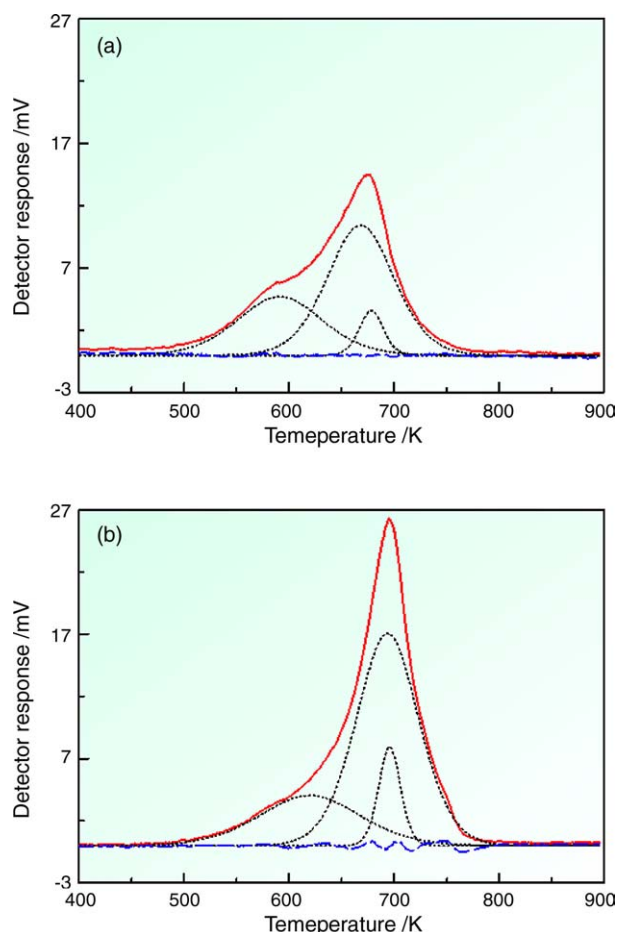


Fig. 4. CO_x formation profiles during TPO of the spent NiMo-C catalyst charged near the inlet (a) and the outlet (b) of the HDS reactor. Curve-fitting results for each profile are also shown in the same figure ((—) observed, (---) fitted and (---) difference).

carbonaceous compounds were further characterized by Raman spectroscopy. In Fig. 5, Raman spectra of the carbonaceous compounds on the spent NiMo-A (i) and NiMo-A (iii) catalysts are shown. Raman spectrum of the graphite is also shown in the same figure as a reference. Raman spectrum of the graphite shows a sharp band and a broad band at 1580 and 1360 cm^{-1} , respectively. These bands are assigned to E2g mode (G band) and A1g mode (D band) of the graphite, respectively. It is well known that G band becomes sharper and stronger with increasing the graphitization of the carbon materials.

Contrary to the spectrum of the graphite, Raman spectrum of the carbonaceous compounds on the spent NiMo-A (i) catalyst shows a broad band ranging from 1600 to 1300 cm^{-1} . A curve fitting analysis using Lorentz-type peak showed that this spectrum is deconvoluted into two peaks positioned at 1560 and 1420 cm^{-1} . Because the higher frequency band was much weaker and broader compared with that observed in the spectrum of the graphite, the carbonaceous compounds deposited on this spent catalyst have an amorphous-like structure. On the other hand, the spectrum of the carbonaceous compounds on the spent

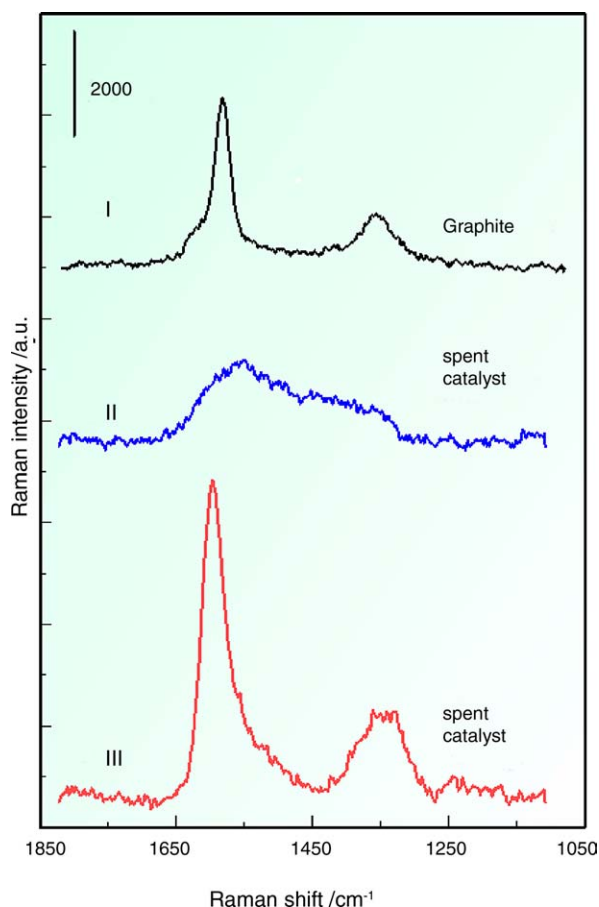


Fig. 5. Raman spectra of carbonaceous compounds deposited on the spent NiMo-A catalysts and reference graphite. The spectra II and III are for the spent NiMo-A (i) and NiMo-A (iii) catalysts, respectively.

NiMo-A (iii) catalyst shows a sharp band at 1580 cm^{-1} and a broad band at 1360 cm^{-1} . Relative intensity, FWHM and band position of these bands are almost the same as those observed in the spectrum of the graphite. Therefore, the carbonaceous compounds deposited on this spent catalyst have a graphite-like structure.

From Figs. 2 and 5, one can see that Raman spectrum of the carbonaceous compounds shows the sharp band at 1580 cm^{-1} if TPO profile shows the presence of the refractory carbonaceous compound. Alternatively, only broad bands appear in Raman spectrum. To relate the combustive properties by TPO to the graphitization degree estimated by Raman spectroscopy, FWHM of Raman band at around 1580 cm^{-1} is plotted against the amount of the carbonaceous compounds having different combustive properties shown in Table 2 and the obtained plot is shown in Fig. 6. FWHM of Raman band around 1580 cm^{-1} shows no clear relation with the amount of the carbonaceous compounds combusted below 680 K during TPO whereas it decreases sharply with increasing the amount of the refractory carbonaceous compound. In other words, a clear relation is found between the combustive property and the graphitization degree of the carbonaceous compound

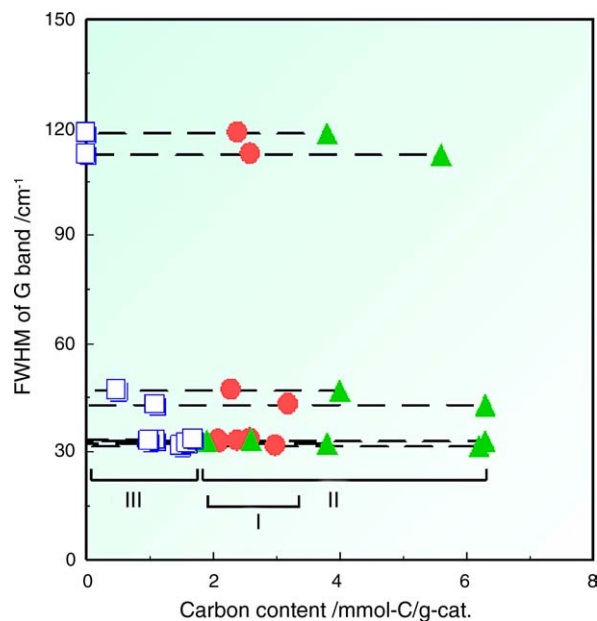


Fig. 6. Relationship between the amount of carbonaceous compounds determined by TPO and FWHM of Raman band. The Roman numerals represent the deconvoluted peaks. They are denoted as I, II and III from low temperature to high temperature (see also Table 1).

irrespective of the catalyst composition and the reaction conditions during ultra-deep HDS of gas oil. This relation indicates that the refractory carbonaceous compound has a graphite-like structure.

3.4. Impact of the deposition of carbonaceous compounds on the catalyst deactivation and its formation mechanism during ultra-deep HDS of gas oil

In our previous study [10], we found that the combustive property of carbonaceous compounds deposited on the spent NiMo-A catalysts changes depending on the reaction conditions employed for ultra-deep HDS of gas oil. Furthermore, it was found that the residual HDS activity of the spent catalysts decreases with increasing the amount of the refractory carbonaceous compound that is combusted at around 690 K during TPO–GC. Therefore, we suggested that the deposition of the refractory carbonaceous compound is one of main reasons for the catalyst deactivation. In the present study, we have also found that this type of carbonaceous compound is deposited on the spent NiMo-B, NiMo-C and NiMo-D catalysts as well. Besides, we have found a simple correlation between the amount of the refractory carbonaceous compound and FWHM of Raman band at around 1580 cm^{-1} for all the spent catalysts examined here, i.e. the greater the amount of the refractory carbonaceous compounds is, the sharper Raman band is. These findings suggest that the deposition of the carbonaceous compound having a graphite-like structure is one of main reasons for the deactivation of NiMo catalyst during ultra-deep HDS of gas oil.

In order to understand why the carbonaceous compound with a higher graphitization degree is more deleterious to the catalyst, we further estimate the lateral size of the carbonaceous compounds (L_a value) from the following equation [13,14].

$$L_a \text{ (nm)} = 4.4 \frac{I_G}{I_D}$$

I_G and I_D in the above equation indicate the integrated intensities of G and D bands in Raman spectrum, respectively. In Fig. 7, L_a value thus estimated is plotted as a function of FWHM of Raman band at around 1580 cm^{-1} . From this figure, we can see that L_a value of the carbonaceous compound seems to increase with decreasing FWHM, indicating that the carbonaceous compound with a higher graphitization degree possesses a greater lateral size. de Jong et al. [15] investigated the graphitization degree of the carbonaceous compounds deposited on CoMo and Mo catalysts used for the HDS of VGO by Raman spectroscopy and found that the carbonaceous compound deposited on the spent CoMo catalyst has a higher graphitization degree than that on the spent Mo catalyst. Their XPS analysis furthermore indicated that the surface coverage of the carbonaceous compound on the spent CoMo catalyst is higher than that of the carbonaceous compound on the spent Mo catalyst at the similar carbon content. Because BET surface area of these catalysts is almost similar, their results suggest that the carbonaceous compound having the graphite-like structure tends to be spread out over the catalyst surface rather than piling up. Taking the work by de Jong et al. into consideration, we suggest from Fig. 7 that the carbonaceous compound with a higher graphitization degree can cover the catalyst surface more effectively than the amorphous-like

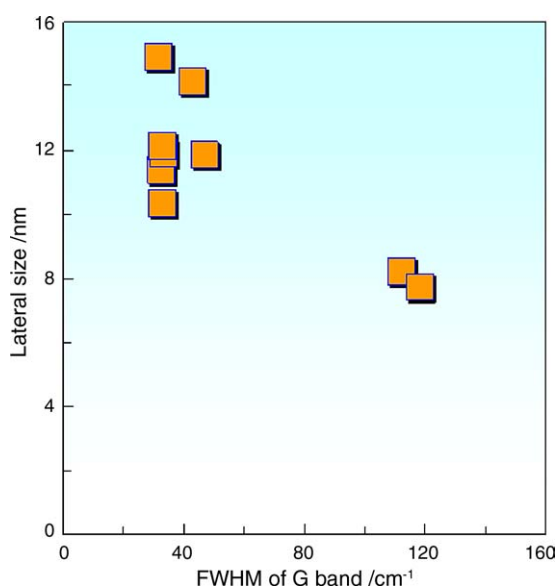


Fig. 7. Relationship between FWHM of Raman band and the lateral size of the carbonaceous compounds estimated from the relative intensities of Raman bands [13].

one, which may lead to more severe catalyst deactivation although it is unclear at present what kinds of catalytic component are covered with these carbonaceous compounds.

As concerned with the formation mechanism of such the carbonaceous compound, it is worthy to note here that the amount of the refractory carbonaceous compound increases with increasing both 90% distillation temperature of the feed gas oil and the maximum reaction temperature in the case of the spent NiMo-A catalysts whereas no clear relationship was observed between the amount of the refractory carbonaceous compound and the days on-stream [10]. Therefore, we suggested that the refractory carbonaceous compound is formed through the adsorption of a heavy molecule(s) originally contained in the feed gas oil. Higher reaction temperature will facilitate the polymerization and graphitization of the adsorbed molecules. However, the present study has found that this type of the carbonaceous compound is preferentially observed on the catalyst charged near the outlet of the HDS reactor. It should be noted that the reaction temperature employed for ultra-deep HDS of gas oil was kept constant along with the axis of the reactor. Therefore, it is more likely that the heavy molecule(s) in the feed gas oil is suffered from structural changes during passing through the HDS reactor, which is then adsorbed on the catalyst surface and converted into the carbonaceous compound with a higher graphitization degree during ultra-deep HDS of gas oil.

4. Conclusions

The present study investigated the combustive properties and structures of the carbonaceous compound deposited on NiMo/Al₂O₃ catalyst that had been used for ultra-deep HDS of several gas oils at various conditions by both TPO–GC (MS) and Raman spectroscopy. Combining with the results obtained in our previous study, we discuss the structure of the carbonaceous compound in relation to the catalyst deactivation and its formation mechanism. The important results obtained in the present study are summarized as follows:

1. A curve fitting analysis of TPO–GC profiles shows that the carbonaceous compounds combusted below 680 K during TPO are observed on all the spent catalyst examined here whereas a refractory carbonaceous compound was observed on the catalyst that had been experienced severe HDS reaction conditions.
2. More refractory carbonaceous compound is observed on the catalyst charged near the outlet of the HDS reactor. This suggests that the precursor for this type of carbonaceous compound is not directly formed from the feed gas oil, but is indirectly formed during the HDS of the feed.
3. Raman spectra of the carbonaceous compounds indicate that the refractory carbonaceous compound has a

graphite-like structure whereas the carbonaceous compound combusted below 680 K during TPO has an amorphous-like structure.

4. The carbonaceous compound having a graphite-like structure possesses a greater lateral size than the amorphous one, implying that the refractory carbonaceous compound can cover the catalyst surface more effectively than the amorphous one.

Acknowledgements

This study was supported by Industrial Technology research Program in '04 from New Energy and Industrial Technology Development Organization (NEDO) of Japan.

References

- [1] M. Egorova, R. Prins, *J. Catal.* 224 (2004) 278.
- [2] NEDO Activity Report, "Research and Development of Petroleum Refining Pollutant Reduction", 2002, pp. 82–161.
- [3] M. Yamada, *Shokubai* 43 (4) (2001) 276–281.
- [4] B.S. Clausen, H. Topsøe, F.E. Massoth, in: J.R. Anderson, M. Boudart (Eds.), *Catalysis Science and Technology*, vol. 11, Springer, 1996.
- [5] R. Koide, S. Fukase, A. Al-Barood, K. Al-Dolama, A. Stanislaus, M. Absi-Halabi, in: B. Delmon, G.F. Froment (Eds.), *Catalyst Deactivation*, Elsevier Science B.V., 1999, pp. 419–422.
- [6] M. Marafi, S. Stanislaus, *Appl. Catal. A: Gen.* 159 (1997) 259–267.
- [7] J. van Doorn, J.L. Bosch, R.J. Bakkum, J.A. Moulijn, in: B. Delmon, G.F. Froment (Eds.), *Catalyst Deactivation*, Elsevier Science B.V., 1987, pp. 391–402.
- [8] P. Zauthen, P. Blom, B. Muegge, F.E. Massoth, *Appl. Catal.* 78 (1991) 265–276.
- [9] M.A. Callejas, M.T. Martinez, T. Blasco, E. Sastre, *Appl. Catal. A: Gen.* 218 (2001) 181–188.
- [10] N. Koizumi, Y. Urabe, K. Hata, M. Shingu, K. Inamura, Y. Sugimoto, M. Yamada, *J. Jpn. Petrol. Inst.* 48 (4) (2005) 204–215.
- [11] F.E. Massoth, *Fuel Process. Tech.* 4 (1981) 63–71.
- [12] P. Zeuthen, B.H. Cooper, F.T. Clark, D. Arters, *Ind. Eng. Chem. Res.* 34 (1995) 755–762.
- [13] K. Kinoshita, *Carbon Electrochemical and Physicochemical Properties*, A Wiley-Interscience Publication, 1988, pp. 115–123.
- [14] T. Itoh, K. Abe, M. Mohamedi, M. Nishizawa, I. Uchida, *J. Solid State Electrochem.* 5 (2001) 328–333.
- [15] K.P. de Jong, D. Reinalda, C.A. Emeis, in: B. Delmon, G.F. Froment (Eds.), *Catalyst Deactivation*, Elsevier Science B.V., 1994, pp. 155–166.